Influence of SiO_2 Crystallinity and Impurities on the Reactivity of Lime-Silica Mixtures

K. Baltakys[1], R. Jauberthie[2], R. Siauciunas [1]

[1]Department of Silicate Technology, Kaunas University of Technology, Radvilenu 19, LT – 50270 Kaunas, Lithuania

[2]Department of Civil Engineering, INSA, 20 Av. des Buttes de Coësmes, CS 14315, 35043 Rennes, France

Corresponding author. Tel.: +370 37 300150; fax: +370 37 300152.
E–mail address: kestutis.baltakys@ktu.lt (K.Baltakys)

ABSTRACT

Several industrial by-products (Hi-Silica, thermal silica densified) were characterized from the chemical and mineral viewpoint and investigated their interactions with portlandite at 180 and 200 ^oC. The molar ratio of primary mixture was $CaO/SiO_2 = 0.66$. The duration of the reaction varies from 24 to 168 hours. The phase composition and properties of calcium silicate hydrates is strongly affected by crystallinity and impurities in SiO_2. It was determined that silica fume – Hi-Sil contains a large quantity of absorbed water which retarded the reaction between lime and SiO_2. Low-base calcium silicate hydrates form more heavily comparing with pure system. Carbon impurities in silica thermal densified influences reactivity of initial mixture and impede reaction between Ca^{2+} and Si^{4+} ions. It was found that reactivity of silica thermal densified significantly increased after burning it at 900 ^oC and became suitable as raw material for the synthesis of calcium silicate hydrates. Meanwhile, in the lime–quartz– H_2O system, due to low quartz solubility rate even in 168 hours of synthesis at 200 ^oC the main products are 1.13 nm tobermorite and xonotlite. Obtained results were confirmed by XRD, DSC, IR and SEM analysis methods.

Keywords Portland cement, silica fume, lime-silica reactivity, low base calcium silicate hydrates, X-Ray diffraction, France.

1. INTRODUCTION

Silica fume (SF), an anhydrous amorphous silica formed at high temperature and collected from the gas phase at voluminous, extremely finely divided powders (Ralph, 1979). Benefits realized when utilizing SF include (Gautefall, 1986; Radjy, 1986; Kohno, 1989; Yamato, 1989; Marusin, 1989): substantial increases in compressive strength of concrete while maintaining the same mixing parameters (the ratio of cement/sand); reduction in the required cement content for a specific target strength; and increased durability of hardened concrete when added in optimum amount.

The interaction of microsilica with Portland cement has been the subject of numerous detailed investigations (Report of a Concrete Society Working, 1993; Working Group on Condensed Silica Fume in Concrete, 1988; Mehta *et al*., 1982). There are three separate effects caused by

the addition of microsilica to cement: a pozzolanic reaction, together with active and passive filler effects. These can function both independently and synergistically.

The actual mechanisms by which SF improves the concrete behavior are still under discussion. Certainly an improvement of the microstructure, i.e. pore refinement, leads to an increase of the concrete strength. Other properties were modified: low capillarity and permeability, low carbonation, high durability with frost, low alkali reaction and sulfatation. If silica fume is added to the cement paste both the total porosity is reduced (Khan *et al.*, 2000) and the pore structure is refined (Li *et al.*, 1996). Another very important effect of silica fume that was found experimentally (Scrivener *et al.*, 1988) and confirmed by numerical simulation (Bentz *et al.*,1991), is the improvement of the interfacial transition zone between aggregates and cement paste. Moreover, it is well documented in the literature that the use of silica fume in concrete results in a significant improvement in the mechanical properties of concrete, but researchers are yet to arrive at a unique conclusion regarding the optimum silica fume replacement percentage (Babu *et al*., 1994; Sabir, 1997; Mazloom *et al*., 2004). A number of researchers have reported different replacement levels as optimum for obtaining maximum strengths of concrete (Bhanja *et al*., 2005; Mansour, 2004).

The principal effects of silica-fume on microstructure of concrete are due to the pozzolanic reaction and to the filler-effect due to particle dimension, being the average silica-fume particle size (0.1 μm) one order of magnitude smaller than the cement particle size. By adding SF to the fresh mix, it is also possible to improve the workability and decrease or avoid bleeding (Neville, 1995; Aïtcin, 1998).

As a pozzolana, SF reacts with calcium hydroxide (CH) liberated by the hydrolysis of C_3S and C_2S of Portland cement. The CH constitutes about 20–25 % of the volume of the hydration products and CH crystals grow in solution. Due their morphology, they are relatively weak, brittle and not cementitious. Cracks can easily propagate through regions populated by CH crystals, especially at the aggregate cement paste matrix interface. The percentage of CH consumed by SF is represented as an index of the pozzolanic activity of SF. It has been reported that due to high pozzolanic action of SF, about 25 % of SF consumes most of liberated $Ca(OH)_2$ at about 28 days. The reaction process is given by the following equations:

$2C_3S + 6H \quad C_3S_2H_3 + 3CH$

Portland cement

$2C_2S + 4H \longrightarrow C_3S_2H_3 + CH$

Silica fume

$3CH + 2S \longrightarrow C_3S_2H_3$

However, some modifications of SF are polluted with various impurities, which significantly or completely prevent the latter reaction. These additives not even unimproved concrete properties but often worsen it. Moreover, the hardening of Portland cement proceeds quite long time and the investigation of influence of SF impurities to the reaction mechanism is very complex. This process can be accelerated when SF interaction with $Ca(OH)_2$ is carried out in the hydrothermal conditions.

The aim of this research is to characterize several industrial by-products from the chemical and mineral viewpoint and to investigate their interactions with portlandite in the hydrothermal conditions. But mechanical approach, applications in mortar composites and long term reactions like 28 days or more were not considered in this paper. As it is well know, the temperatures used in this work influence the kinetic of reactions. In a second way, it was necessary to control at low temperature and long term conduct to the same minerals.

2. MATERIALS AND METHODS

The following raw materials were used in this work: calcium hydroxide $Ca(OH)_2$ (Industrial lime: loss of ignition 23%, Manufacturer Pigeon Chaux, Saint Pierre La Cour, FRANCE); two different silica fume (Hi-Sil 255C-D obtained from PPG and thermal silica densified – TSD); quartz (from Millisil Sifraco). Both the raw materials and products of hydrothermal synthesis were characterized by X-ray powder diffraction (XRD), differential scanning calorimetry (DSC), thermogravimetry (TG), FT-IR spectroscopy (FT-IR) and scanning electron microscopy (SEM) analysis.

The XRD data were collected with Philips PW 3710 X-ray diffractometer with Bragg–Brentano geometry using Ni-filtered Cu K_α radiation, operating with the voltage of 30 kV and emission current of 20 mA. The step-scan covered the angular range 2–60^o (2θ) in steps of $2\theta = 0.02^o$, 2s by step.

Simultaneous thermal analysis (STA: differential scanning calorimetry–DSC and thermogravimetry–TG) was also employed for measuring the thermal stability and phase transformation of synthesized products at a heating rate of 15 ^{o}C/min, the temperature ranged from 30 ^{o}C up to 1000 ^{o}C under the air atmosphere. The test was carried out on a Netzsch STA 409 PC Luxx instrument. The ceramic sample handlers and crucibles of Pt-Rh were used there.

SEM (JEOL-JSM-6301F) analysis was performed of the samples using an accelerating voltage of 9 kV and a working distance of 15 mm.

FT-IR spectra has been carried out with the help of spectrometer Perkin Elmer FT–IR system Spectrum X. Specimen were prepared by mixing 1 mg of the sample with 200 mg of KBr. The spectral analysis was performed in the range of 4000–400 cm^{-1} with spectral resolution of 1 cm^{-1}.

Firstly, the surface texture and morphology of by-products were investigated by performing SEM analysis. It was determined that Hi-Sil is a very fine powder with spherical particles (smaller in size than Portland cement or fly ash). As showed in Fig. 1 (a), the agglomerates consist of many ultra-fine silica fume grains. The diameters of particles varies in the range of 20–50 nm.

Meanwhile, the morphology of TSD differs from Hi-Sil: this material consists of much lager separated particles with diameters in the range from 50 to 200 nm (an average of 100 nm) (Fig. 2, a).

FT-IR studies were conducted to identify the structure and nature of amorphous silica in both types of pozzolan. The spectrum of Hi-Sil shows the strongest absorbance bands at 1107, 801, and 472 cm^{-1}, characteristic of condensed silica (Fig. 1, b). The broad band centered at 1107 cm^{-1} is attributed to asymmetric stretching frequency of Si–O–Si, the band centered at 801 cm^{-1} is due to symmetric stretching of Si–O–Si, and the band at 472 is due to the bending frequency of O–Si–O. The frequencies of the Si–O–Si bands are an indication of the overall degree of polymerization of the silica network. In general, a lower frequency will correspond to a lower degree of polymerization. Thus, the degree of polymerization of Hi-Sil is a lower comparing with TSD because the latter material corresponding absorbance bands are at 1120, 808, 479 cm^{-1}. The band at 967 cm^{-1} due to the Si–O stretching mode of nonbriding oxygens. The former band also confirms the lower degree of polymerization of silica in Hi-Sil comparing with TSD (Fig. 2, b). The band at 1631 cm^{-1} is due to the H–O–H bending vibration of molecular H_2O and the broad band at 2800–3700 cm^{-1} is due to the stretching vibration of –OH groups in H_2O hydroxyls with a wide range of hydrogen bonding strengths.

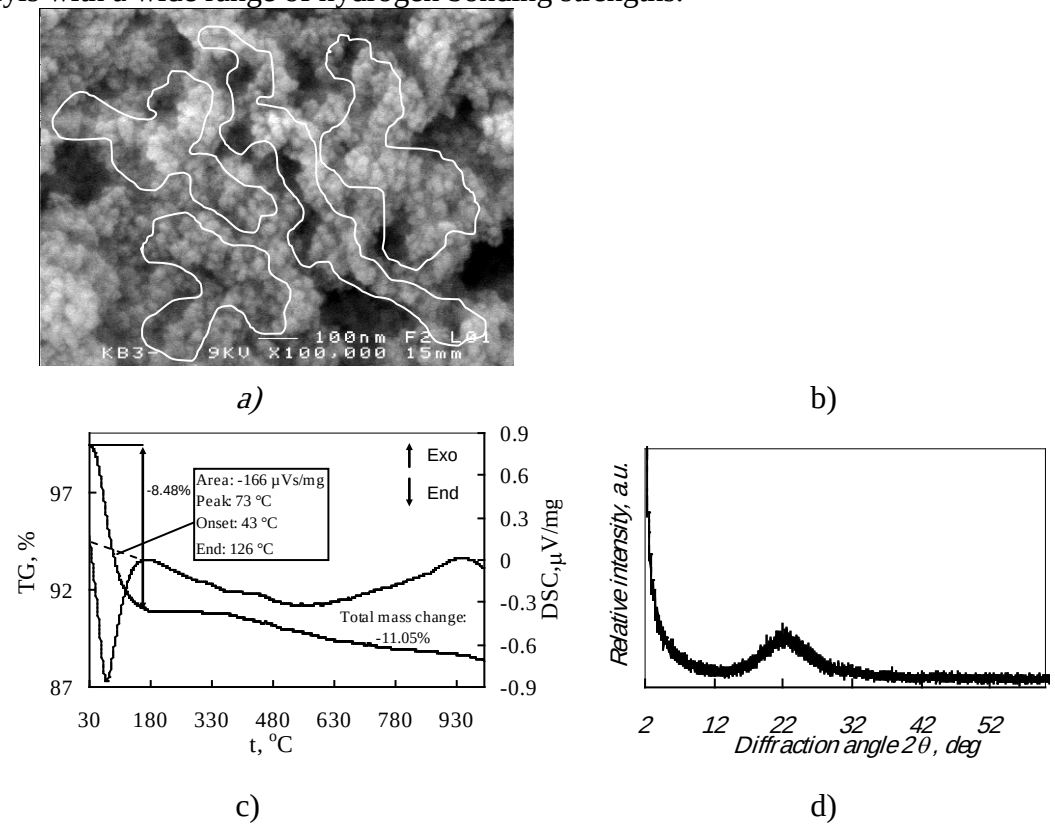

Figure 1**.** SEM photograph (a), FT-IR spectrum (b), DSC-TG curves (c) and XRD pattern (d) of Hi-Sil.

The absorption bands account for the noticeable large loss on ignition of Hi-Sil, which results from the loss of hydrogen bonded water (Si–OH:OH_2). The hydrogen bonded water may still persist in the silica gel until 200°C (Vincente *et al.*, 1996), and in some cases up to 500°C (Chuang *et al.*, 1997), if it is strongly hydrogen bonded to opposite sides of the pore walls. These results were confirmed by DSC analysis.

In the case of Hi-Sil, TG data shows that the main weight loss (8.48 wt %) occurs between 30 and 175 ^{o}C, when a total mass change is equal 11.05 % (Fig. 1, c). The DSC curve has a broad endothermic peak (166 μV/mg) centered at about 73 ^{o}C. It should be underlined that this endothermic peak is associated with the loss of absorbed water from Hi-Sil structure.

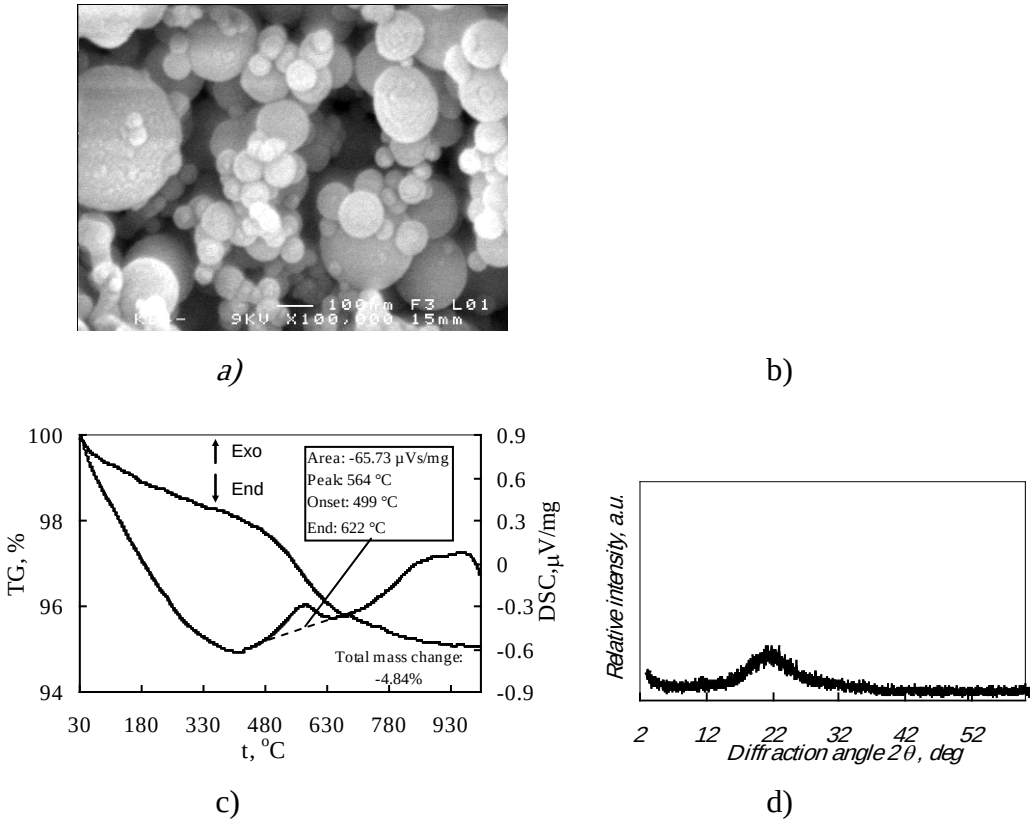

Figure 2. SEM photograph (a), FT-IR spectrum (b), DSC-TG curves (c) and XRD pattern (d) of thermal silica densified

Meanwhile, the DSC-TG profile of TSD differs to compare with Hi-Sil: in the temperature range from 30 to 420 ^{o}C the mass loss is very small (1.51 wt %) and no remarkable peaks were detected in DSC curve (Fig. 2, c). This fact indicates that TSD contains very small amount of absorbed water. However, at higher temperatures (above 450 ^{o}C), the DSC curve has a broad and large exothermic peak (65.73 μV/mg) centered at about 564 ^{o}C. This effect is associated with carbon combustion when mass loss is equal 2.51 wt % (Fig. 2, c).

XRD analysis of both SF show only the hump associated with amorphous SiO_2 (centered at 2θ = 22 °). The diffraction patterns are given in Fig. 1 and 2 (d).

All characteristics of quartz greatly differ from both SF: figure 3 (a) presents irregularly oriented plate-like crystals of quartz with diameters in the range from 200 nm to 2 μm (an average of 1 μm). It should be noted that quartz sample shows a strong absorption bands in the range 70–790

cm^{-1} (Fig. 3, b). The DSC endotherm of quartz identifies inversion of alpha-quartz into beta-quartz at 579 °C (Fig. 3, c) and X-ray diffraction pattern of this sample shows basic reflections of crystalline material characteristic referring to this compound (Fig. 3, d, *d*-spacing–0.425; 0.334; 0.245; 0.228 nm).

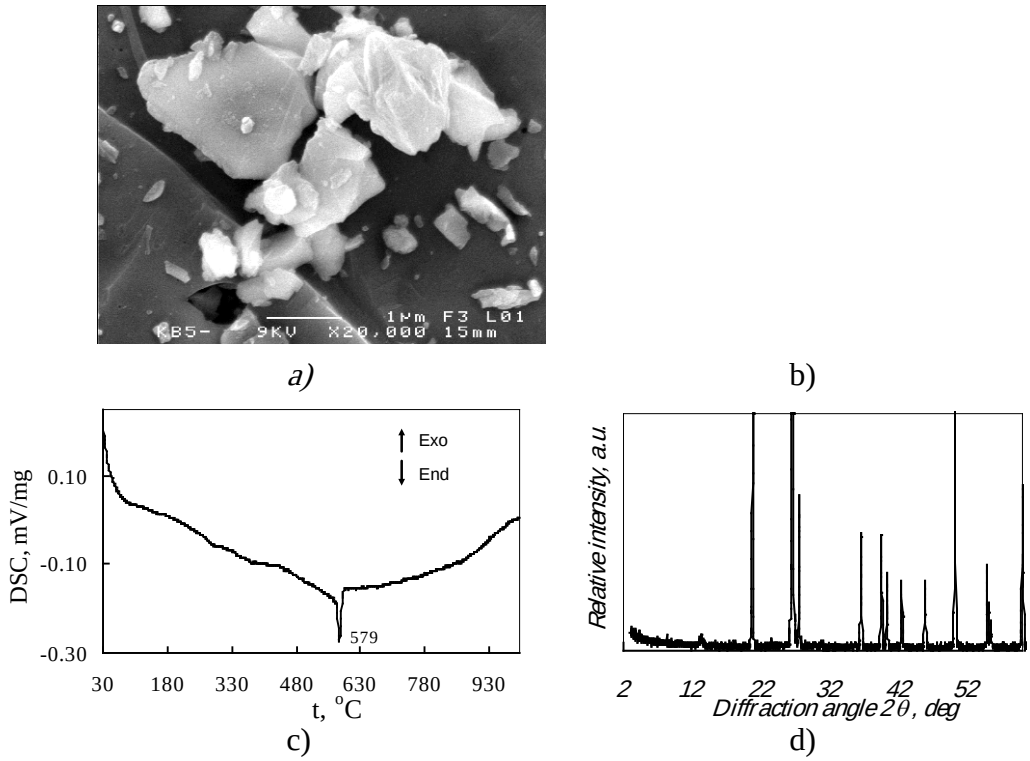

Figure 3. SEM photograph (a), FT-IR spectrum (b), DSC curve (c) and XRD pattern (d) of quartz

The products of synthesis are obtained by hydrothermal reaction of $Ca(OH)_2$ and different SiO_2 or $Si(OH)_4$. The molar ratio of primary mixtures was $CaO/SiO_2 = 0.66$. The synthesis has been carried out in teflon cells placed in sealed bombs heated to 180 and 200 °C, under pressure of saturated water vapour. The duration of the reaction varies from 24 to 168 hours. At the end of the experiment, the bombs are hardened in water at 20 °C and the products were then transferred to an air conditioned chamber with relative humidity of 55 % and temperature of 20 °C.

3. RESULTS AND DISCUSSIONS

The effect of crystallinity and impurities in SiO_2 on the reactivity of lime-silica mixtures was determined. In the lime–Hi-Sil–H_2O mixture, after 96 hours of synthesis at 180 °C the formation of quite good crystalline Z-phase (Fig. 4, curve 1, *d*-spacing–1.475; 0.823; 0.412; 0.378; 0.303; 0.182 nm; exothermic effects at 82 and 142 °C) and C-S-H(I) (*d*-spacing–0.303; 0.182 nm) were observed (Fig. 4, curve 1, endothermic effect at 834 °C). These results differ from previous experiments (Siauciunas *et al.,* 2004) in which reagent $SiO_2 \cdot H_2O$ was used.

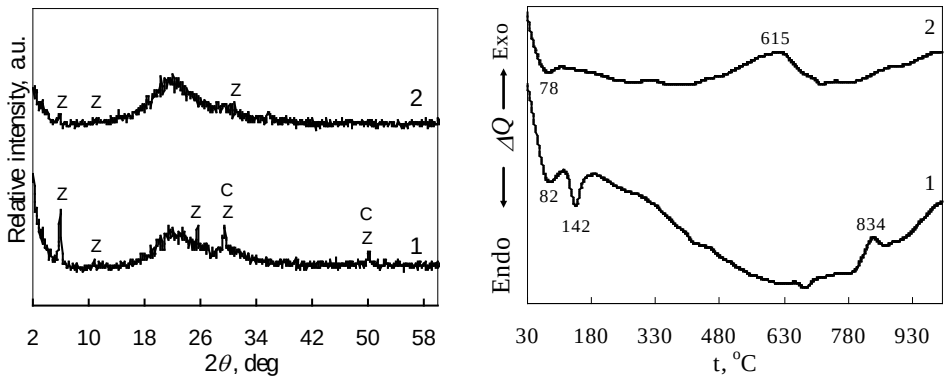

a) b)

Figure 4. X-ray diffraction patterns (a) and DSC curves (b) of synthesis products when duration of hydrothermal curing at 180 ^{o}C is equal 96 h. SiO_2 components: curve 1 – Hi-Sil, curve 2 – TSD. Indeles: Z – Z-phase, C – C-S-H(I).

Z-phase tends to crystallize in clusters of irregular plates, while C-S-H(I) is the fibrous material, the fibres are being up to about 2 μm long (Fig. 5, a).

While at the same time, in the lime–TSD–H_2O system, the formation of calcium silicate hydrates proceed very difficult. The main reason is that TSD contains large quantity of carbon which impedes reaction between Ca^{2+} and Si^{4+} ions (Fig. 2, b, exothermic effect at 615 ^{o}C). Due to this reason, in the products only the traces of Z-phase formed and large quantity of unreacted TSD remained (Fig. 5, b). It should be noted that exothermic peak of C-S-H(I) is not remarkable in DSC curve (Fig. 4, b, curve 2). Thus, carbon exists between TSD grains and prevents synthesis of poorly ordered gel (C-S-H gel, gyrolite gel, tobermorite gel).

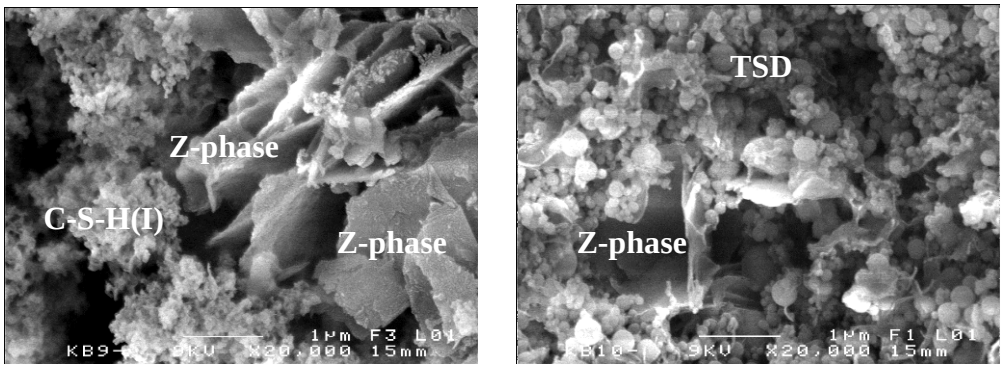

a b

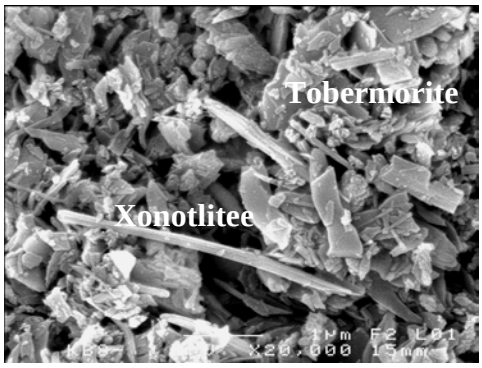

c

Figure 5. Scanning electron micrographs of synthesis products when duration of hydrothermal curing at 180 ^{o}C is equal 96 h. SiO_2 components: a – Hi-Sil, b – TSD, c – quartz.

Gyrolite synthesis in the lime–quartz–H_2O system with $CaO/SiO_2 = 0.66$ proceed very heavily: even after 96 hours of isothermal curing at 180 ^{o}C in the products dominate 1.1 nm tobermorite and small quantity of quartz remain. It should be underlined that tobermorite is not stable and starts to transform into xonotlite. SEM identifies the two distinct morphologies of the calcium silicate hydrates: the plate-like tobermorite crystals are visible intergrown at or near fibrous shaped crystals of xonotlite (Fig. 5, c).

By the way, the same experiments were carried out in duration of 168 h and obtained results showed no differences comparing to previous data.

In order to intensify the formation of low-base calcium silicate hydrates, we increased the temperature of isothermal curing up to 200 ^{o}C.

In the lime-Hi-Sil mixture, after 24, 48 h of synthesis alone C-S-H(I) type calcium silicate hydrate dominated (Fig. 6, curve 1). Only after 96 hours of hydrothermal curing, as well as at 180 ^{o}C, well-crystallized Z-phase crystals and traces of C-S-H(I) are noticed (Fig. 6, curve 2). It should be underlined that Z-phase at 200 ^{o}C temperature transforms into gyrolite gel only after 168 h (Fig. 6, curve 3).

The DSC analysis confirmed the obtained XRD results: at 200 ^{o}C after 168 h synthesis the clear endothermic peak at 130–140 ^{o}C and exothermic peak at 820–840 ^{o}C characterizing low-base calcium silicate hydrates were obtained.

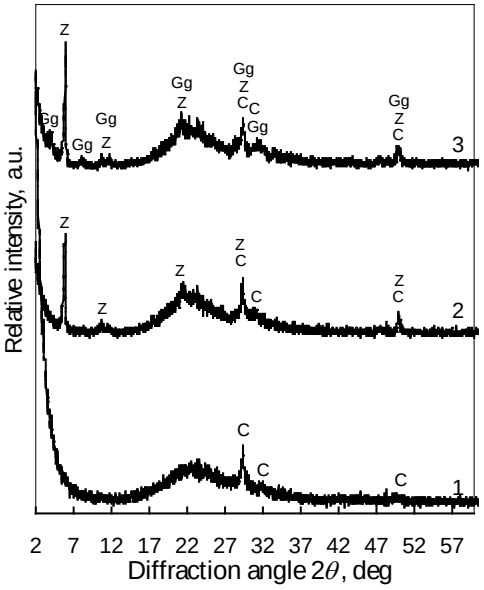

Figure 6. X-ray diffraction patterns of synthesis products when SiO_2 component–Hi-Sil. Duration of hydrothermal synthesis at 200 ^oC: 1 – 48 h, 2 – 96 h; 3 – 168 h. Indexes: C – C-S-H(I); Z – Z-phase; Gg – gyrolite gel;

In the lime–TSD mixture at 200 ^oC, gyrolite formation reactions proceed as well as difficult: only after 168 h of isothermal curing traces of gyrolite gel together with Z-phase were found (Fig. 7).

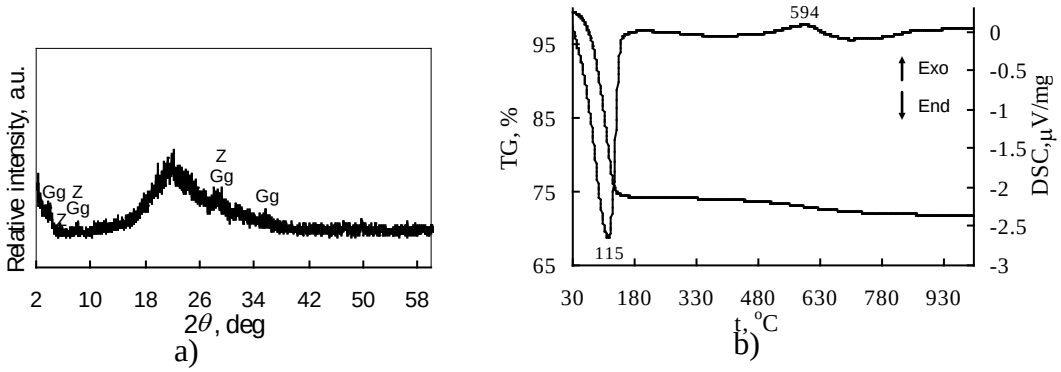

Figure 7. X-ray diffraction patterns (a) and DSC curves (b) of synthesis products when SiO_2 component – TSD. Duration of hydrothermal synthesis at 200 ^oC is 168 h. Indexes: Gg – gyrolite gel, Z – Z-phase.

It should be pointed out that in CaO–quartz–H_2O system, due to low quartz solubility rate in the reacting mixture C/S ratio is higher than 0.66 besides already after 24 hours of isothermal curing at 200 ^oC, xonotlite forms together with 1.13 nm tobermorite and quite large quantity of quartz remains. At longer time of synthesis (168 h) although quartz dissolves completely, but the same basicity calcium silicate hydrates – xonotlite and 1.13 nm tobermorite were observed (Fig. 8). Xonotlite shows a single, sharp peak in the IR spectrum (Fig. 8, b) at about 3615 cm^{-1} which can

be assigned to structural (OH), and a further sharp peak at 1204 cm^{-1} which is due to the stretching vibration of the bridging Si-O-Si bonds in the silicate double chains. Meanwhile, tobermorite shows a broad band at 3484 cm^{-1} due to molecular water and a further water peak at about 1636 cm^{-1}. In the DSC spectrum broad endothermic hump occurs at 219 ^{o}C due to molecular water in tobermorite structure and followed by a small exothermic peak at 856 ^{o}C which is characteristics of C-S-H(I) (Fig. 8, c). SEM data confirmed these results (Fig. 8, d).

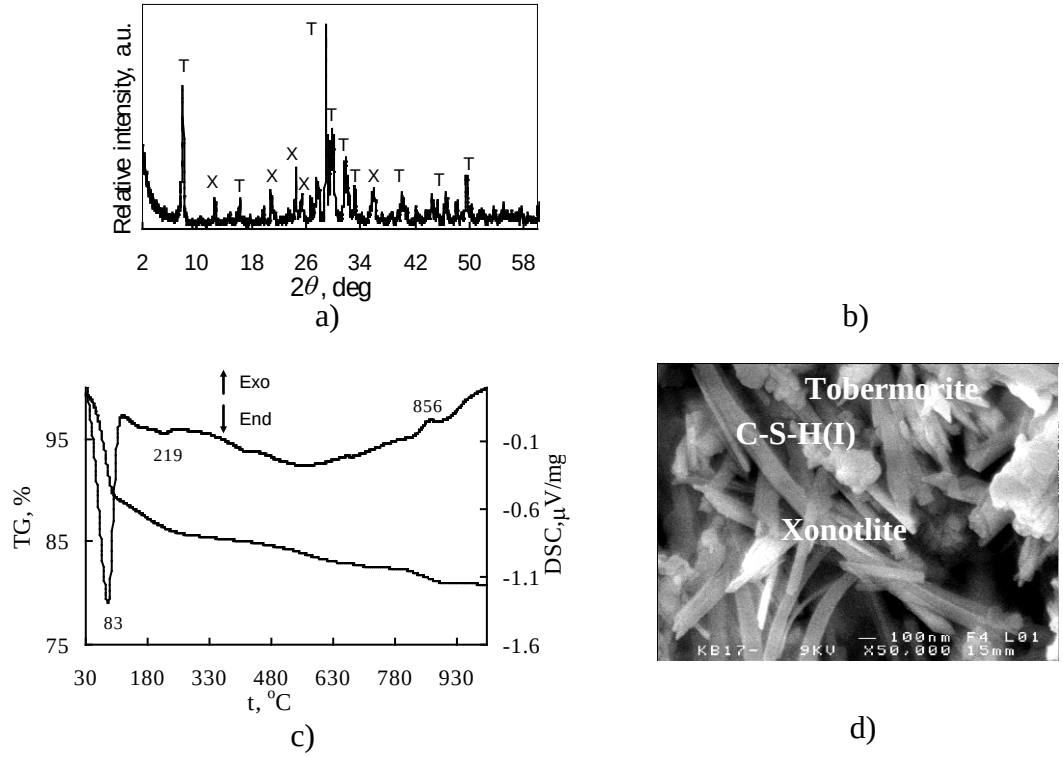

Figure 8. XRD pattern (a), FT-IR spectrum (b), DSC-TG curves (c) and SEM photograph (d) of synthesis products when SiO_2 component – quartz. Duration of hydrothermal synthesis at 200 ^{o}C is 168 h. Indexes: T– tobermorite; X – xonotlite.

It is known (Baltakys *et al.,* 2005) that some admixtures are not recommendable for the synthesis of gyrolite, because they stimulate others calcium silicate hydrates formation and prolong the time of their existence. In this work used Hi-Sil partly consists of SiO_2 or $Si(OH)_4$ and contains a large quantity of absorbed water too. Meanwhile, TSD contains big amount of carbon. In order to eliminate influence of these factors, we heated up both silica fume for 2 hours at 900 ^{o}C temperature. SF properties and the size of particles exchanged: the particles of Hi-Sil become closely linked because between them disappeared slicks of water (Fig. 9, a).; the small particles of TSD were separated by carbon, so after heating already possible to indicate agglomerates (Fig. 9, b). Later on, both heated up SiO_2 modifications were mixed with lime preparing the mixtures with C/S=0.66 and hydrothermaly treated at the same conditions (96 hours at 180 ^{o}C).

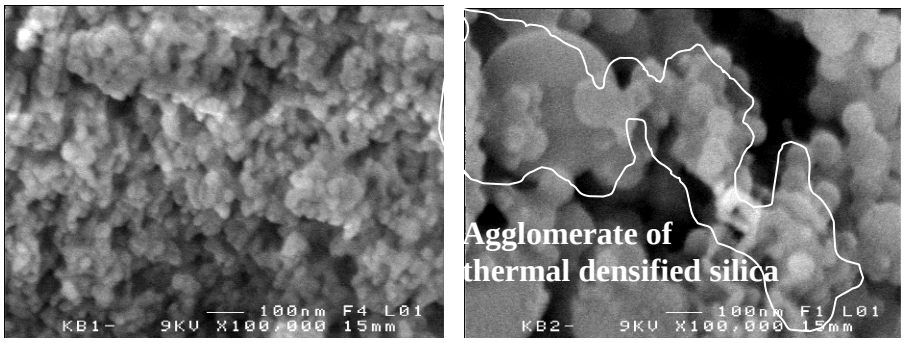

a) b)

Figure 9. SEM photograph of Hi-Sil (a) and TSD (b) after heating up at 900 ^{o}C

As it was expected, in the mixtures with Hi-Sil a larger quantity of more ordered Z-phase together with C-S-H(I) were formed (Fig. 9, a, curve 1). It is presumable that the reaction rate insignificantly increases because after heating the absorbed water was eliminated from Hi-Sil structure.

Meanwhile, using another SiO_2 component–thermal silica densified, the mechanism of compound formation is differ: in the products already gyrolite was dominated and only small quantity of Z-phase was remained (Fig. 9, b, curve 2). Moreover, our research allows to state that after heating TSD become more reactive to compare with Hi-Sil as Z-phase in the pure mixtures forms as the intermediary compound before the crystallization of gyrolite [23, 24].

FT-IR spectroscopy data confirmed SEM and XRD results: doublets near 595 and 614 cm^{-1} characteristics to gyrolite are seen (Fig. 10, d, curve 2). It should be stressed that gyrolite contains greater quantity of molecular H_2O comparing with Z-phase or tobermorite. Consequently, a wide band near 3446 cm^{-1} which correspond to molecular water forms hydrogen bridge links in the interlayers is observed (Fig. 10, d, curve 2). The bands in the range of 1634 cm^{-1} frequency are assigned to $\delta(H_2O)$ vibrations and confirm this presumption.

On the basis of thermal analysis and calculated kinetic parameters it can be concluded that carbon did not participate in the reactions mechanisms of calcium silicate hydrates formation because almost the same quantity of unreacted carbon remains with increasing reaction temperature and/or duration (table 1). It should be underlined that only after 168 h of synthesis at 200 ^{o}C the mass loss a little bit decreases during the combustion of carbon.

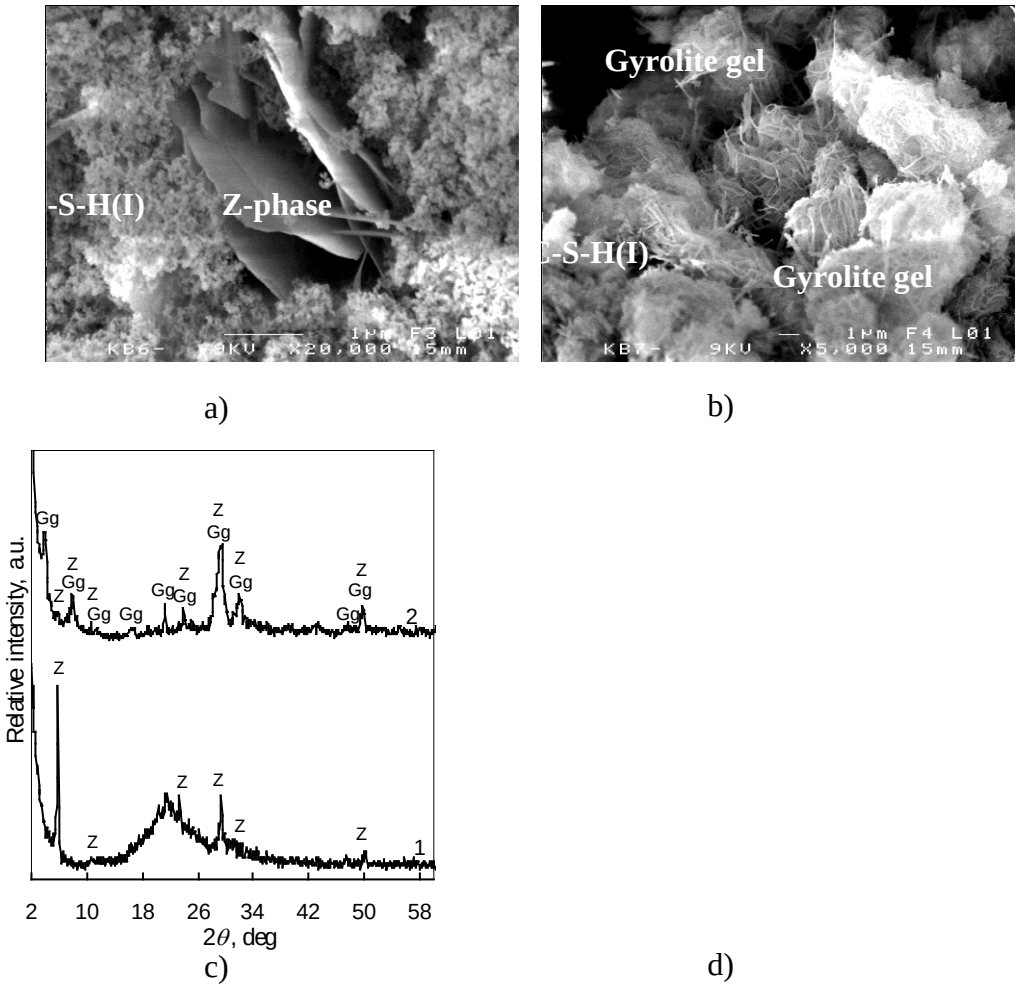

Figure 10. Scanning electron photographs (a, b), XRD patterns (c) and IR spectra (d) of synthesis products when duration of hydrothermal curing at 180 ^{o}C is 96 h. SiO_2 components heated up at 900 ^{o}C:
a – Hi-Sil, b – TSD; curve 1 – Hi-Sil, curve 2 – TSD. Indexes: Z – Z-phase, G – gyrolite gel.

Table 1. Carbon combustion in the temperature range from 450 to 700 ^{o}C with increasing reaction temperature and/or duration

Isothermal curring at 180 ^{o}C	Onset, ^{o}C	Peak, ^{o}C	Area, μVs/mg	Weight loss (%)
96	493	615	65.21	1.91
168	496	610	64.38	1.82
Isothermal curring at 200 ^{o}C				
24	495	605	65.42	1.93
48	500	658	65.68	1.86
96	497	583	65.08	1.91
168	496	593	64.42	1.72

On other hand, the shielding effect carbon strongly influences reactivity of initial mixture and the rate of reaction. This phenomenon can be eliminated by burning SF.

4. CONCLUSIONS

1. SiO_2 modification has deciding influence on the calcium silicate hydrates formation processes. It was determined that silica fume – Hi-Sil contains a large quantity of absorbed water which retarded the reaction between lime and SiO_2, and negatively influence the formation of well-crystalline phases.
2. Carbon impurities in silica thermal densified prevent the formation of new compounds. It was found that reactivity of this material significantly increased after burning it at 900 ^oC and became suitable as raw material for the synthesis of calcium silicate hydrates.
3. It was found that low base calcium silicate hydrates can not be synthesized when a less active but more crystalline modification of SiO_2 – quartz is used. Due to low quartz solubility rate in the products even in 168 hours of synthesis at 200 ^oC 1.13 nm tobermorite and xonotlite were formed.

5. REFERENCES

Aïtcin, P.-C., 1998, High-Performance Concrete, *E&F SPON, London*.

Babu, KG, Rao, GSN., 1994, Early strength of FA concrete. *Cement and Concrete Research*;24:277–84.

Baltakys, K., Šiaučiūnas, R., 2005 09 26 in the press, The influence of Al_2O_3 and Na_2O on the formation of gyrolite in the stirring suspensijon. *Journal of Materials Science*.

Bentz, D.P. & Garboczi, E.J., 1991, Simulation Studies of the Effects of Mineral Admixtures on the Cement Paste-Aggregate Interfacial Zone, *ACI Mater J* 88(5) 518-529.

Bhanja, S, Sengupta, B., 2005. Influence of silica fume on the tensile strength of concrete. *Cement Concrete Res*;35(4): 743–747.

Chuang, S. and Maciel, G.E., 1997, A detailed model of local structure and silanolhydrogen bonding of silica gel surface. J. *Phys. Chem. B*, 101, 3052–3064.

Gautefall, O., 1986, Effects of CSF on the diffusion of chloride through hardened cement paste. Proceedings of the Second International Conference on the Use of Fly Ash, Silica Fume, Slag and Natural Pozzolans in Concrete. Vol. 2, *American Concrete Institute*, SP-91, 991–997.

Khan, M.I., Lynsdale, C.J. & Waldron, P., 2000, Porosity and strength of PFA/SF/OPC ternary blended paste, *Cement and Concrete Research*. 30(8) 1225-1229.

Kohno, K., 1989. Relative durability properties and strengths of materials containing finely ground silica and silica fume. *Proceedings of the Third International Conference on the*

*Use of Fly Ash, Silica Fume, Slag and Natural Pozzolans in Concrete***.** Vol. 2**,** American Concrete Institute, SP-114 , 815–826.

Li, Y., Langan, B.W. & Ward, M.A., 1996, The strength and microstructure of high-strength paste containing silica fume, *Cement Concrete Aggregates* 18(2) 112-117.

Mansour, MY., 2004. Predicting the shear strength of RC beams using ANN. *Engineering Structure*; 26:781–99.

Marusin, S.L., 1989. The influence of length of moist curing time on the weight change behaviour and chloride permeability of concrete containing silica fume. In: Proceedings of the Third International Conference on the Use of Fly Ash, Silica Fume, Slag and Natural Pozzolans. *Concrete, American Concrete Institute*, SP-114 , 924–929.

Mazloom, M., Ramezanianpour, A.A., Brooks, J.J., 2004. Effect of silica fume on mechanical properties of high-strength concrete. *Cement Concrete Composite*; 26: 347–354.

Mehta, P. K. and Gjorv, O. E., 1982, Properties of Portland cement concrete containing fly ash and condensed silica fume. *Cement and Concrete Research*, 12 , 587–595.

Neville, A.M., 1995, Properties of concrete, *John Wiley & Sons*, New York (4th edition).

Radjy, F.F., 1986, A review of experience with condensed silica fume concretes and products. Proceedings of the Second International Conference on the Use of Fly Ash, Silica Fume, Slag and Natural Pozzolans, *Concrete American Concrete Institute, SP-91*, vol. 2, 1135–1152.

Ralph, K.I., 1979, The Chemistry of Silica , *John Wiley & Sons, New York*, 21–29 .

Report of a Concrete Society Working Party, 1993, Microsilica in Concrete, Technical Report No. 41, *Concrete Society*, 1.

Sabir, BB., 1997, Mechanical properties and frost resistance of SF concrete. *Cement Concrete Composite*;19, 285–294.

Scrivener, K.L., Bentur, A. & Pratt P.L., 1988, Quantitative Characterization of the Transition Zone in High Strength Concretes, *Advances in Cement Research* 1(4) 230-237.

Siauciunas, R., Baltakys, K., 2004, Formation of gyrolite during hydrothermal synthesis in the mixtures of CaO and amorphous SiO_2 or quartz, *Cement and Concrete Research*, 34 (11) 2029–2036.

Vincente, M.A., Suarez, M., Lopez-Gonzalez, J.D. and Banares-Munoz, M.A., 1996, Characterization surface area and porosity analyses of the solids obtained by acid leaching of a saponite. Langmuir, 12, 566–572.

Working Group on Condensed Silica Fume in Concrete, 1988, *Condensed Silica Fume in Concrete Thomas Telford, London*, 1.

Yamato, T., 1989, Chemical resistance of concrete containing condensed silica fume. Proceedings of the Third International Conference on the Use of Fly Ash, Silica Fume, Slag and Natural Pozzolanas, *Concrete vol. 2, American Concrete Institute*, SP-114, 897–914.

Abbreviations used

In cement and mortars	In chemical
Hi Sil (manufacturer name)	Amorphous silica
SF (silica fume)	Amorphous silica
H	H_2O
S	SiO_2
C	CaO
CH (portlandite)	$Ca(OH)_2$
C_3S (allite)	$(CaO)_3SiO_2$
C_2S (bellite)	$(CaO)_2SiO_2$
CSH (poorly cristallised tobermorite)	Approximately $(CaOSiO_2H_2O)$
CSH I (poorly cristallised tobermorite)	Approximately (0.8-1.5CaO SiO_2 0.5-2.5H_2O)
$C_3S_2H_3$ (poorly cristallised tobermorite)	Approximately $(CaO)_3(SiO_2)_2(H_2O)_3$

XRD	X Ray Diffraction (powder)
STA	Simultaneous Thermal Analysis
DSC	Differential Scanning Calorimetry
TG	Thermo Gravimetric analysis
FT-IR	Fourrier Transformed Infrared Spectroscopy
SEM	Scanning Electronic Microscopy